Journal of Engineering and Applied Sciences 11 (5): 951-957, 2016
ISSN: 1816-949X

An Investigation of the Seismic Response of a Deck-Type Steel Arch Bridge

[1]Seyyed Ashkan Mostajab Aldavat, [2]Amirhosein Gholizadeh Zahmatkesh,
[3]Selma Teymouri and [4]Majid Barazandeh Tehrani
[1]School of Civil Engineering, College of Engineering, University of Tehran, Tehran, Iran
[2]Tehran University of Science and Culture, Tehran, Iran
[3]Department of Civil Engineering, Islamic Azad University, Damavand Branch, Tehran, Iran
[4]Department of Civil Engineering, IHE Center, University of Applied and Technology, Tehran, Iran

Abstract: This study represents static and dynamic analysis of a steel arch bridge with box section. Steel arch bridge due to the axial bearing of the arch as the main part of the axial bearing has an appropriate mechanism to support vertical loads but when subjected to lateral loads such as earthquakes, they show complex behavior due to the irregularity and lack of lateral stiffness, probability of lateral buckling and etc. In this study, a linear static analysis is performed to determine the maximum amount of shift due to gravity loads preliminary, then a modal analysis is done to better understand dynamic behavior and characterize the dynamic characteristics of the bridge. Also a linear time history analysis is performed using single-component and three-component earthquake excitation records. Time history analysis results including the transverse, longitudinal and vertical recording shifts and maximum compressive axial force as well as bearing reactions in three dimensions are compared in single and three-component record mode.

Key words: Assessment, steel arch bridge, dynamic, seismic, modal analysis, time history

INTRODUCTION

Arch bridges due to the axial bearing of the arch as the main element have an appropriate performance against vertical loads and connecting elements between bridge deck and arch, whether they are located above or below the deck, act axially and use their capacity properly. However when this kind of bridges are affected by the lateral load such as earthquake, arches cannot withstand and transfer lateral loads alone due to the lack of enough lateral stiffness and probability of lateral buckling and for this reason, two arches that are braced are commonly used. Moreover, connecting elements of the bridge deck and arch have not enough bending stiffness and lateral forces induced by earth quake excitation lead to axial forces in these elements. Because of the complex behavior of this kind of bridges compared to the bridges with consecutive bases, far fewer studies have been conducted for seismic assessment of these bridges that have not been enough. Therefore, more studies that are comprehensive are needed for recognizing and predicting the behavior of these bridges under the effect of seismic excitation in order to be able to identify their vulnerable points under the effect of seismic excitation and to propose proper solutions for restoration and rehabilitation of the steel arch bridges.

Torkamani (2002) investigated the dynamic behavior of the braced metal arch bridges using the elastic modeling. Kawashima and Mizoguchi (2000) provided a set of dynamic non-linear analyses in order to study seismic response and performance of an overpass reinforced concrete arch bridge against the strong earthquake in Hyogo-ken. Moreover, Kuranishi and Nakajima (1986) and Sakakibara *et al*. (1998) and Okumura *et al*. (2000) and Yanagi *et al*. (2003) studied the in-plane behavior of the steel arch bridges in which arch is located below the deck against the major earthquake using two-dimensional modeling. This study aims to focus on static and dynamic investigation of Cold Spring Bridge. Comparison of the effect of one-component and three-component acceleration records, maximum joint displacement, maximum axial force of the elements, etc., are discussed in this study. Rehabilitation of the vulnerable areas will be considered in the following studies (Fig. 1).

Cold spring bridge: Cold spring bridge is a steel arch bridge with a box arch section. Likewise, due to the slopes of both sides of the bridge toward each other, irregularity of the bridge is quite evident. This bridge has been selected for comparison of irregularity effect and recognizing the box arch behavior.

Corresponding Author: Seyyed Ashkan Mostajab Aldavat, School of Civil Engineering, College of Engineering, University of Tehran, Tehran, Iran

Fig. 1: A view of cold spring bridge

MATERIALS AND METHODS

Modeling: Modeling of the bridge is based on the information and details provided in Structural Steel Designer's Handbook. In addition, it has been tried to show all effective components (components of main bearing) in the study by analysis of the real photo of the bridge. Based on the information in Structural Steel Designer's Handbook, there is a connection of two sides of the arch with hinged support. The length of the arch span is 700 ft and longitudinal slope of the bridge is 6.6% and the extended uniform live load and dead loads are 9475 and 904 lb/ft, respectively.

Figure 2 shows the model provided by the SAP2000 Software. The connection of the deck beams with the hinged support on one side and shows no thermal stress of the roller on the other hand and elements of beam and shell have been used.

Analysis

Static analysis: Deformation due to extended uniform live load and dead load is shown in Fig. 3. As shown in Fig. 3, deformation of the bridge will be under symmetrical and asymmetrical loads due to the asymmetry of the height of the bridge. Figure 3 shows maximum deformation point in vertical direction has been demonstrated. Figure 4 shows axial force in the parts due to live load and dead load is shown. Force distribution is continuous along the arch. By approaching the end of the arch (right side), axial force of the arch increases.

Modal analysis: The main mode of traverse vibration of the structure is the first mode of vibration with frequency period 1.7244 sec, the main mode of the longitude vibration is the mode No. 27 with frequency period 0.198806 sec and the main mode of vertical vibration is the mode No. 6 with frequency period 0.482444 sec (Fig. 4-8).

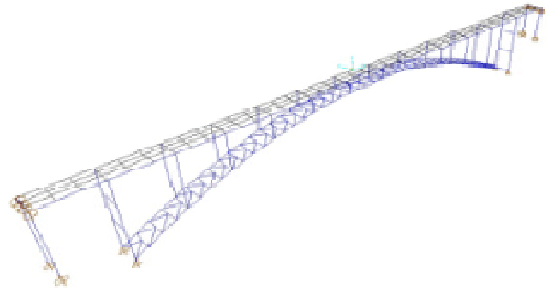

Fig. 2: Model of the bridge

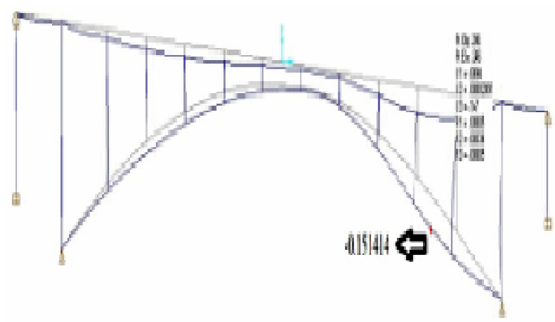

Fig. 3: Deformation due to the extended uniform live load and dead load

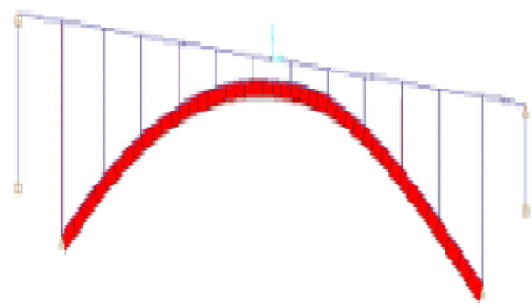

Fig. 4: Axial force under the influence of live load and dead load

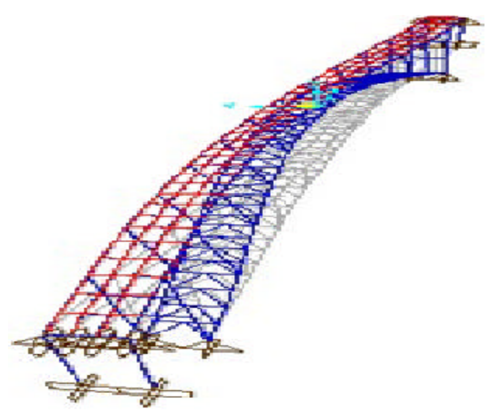

Fig. 5: Bridge deformation in mode no. 1 with frequency period 1, 7244 s-main mode-traverse vibration

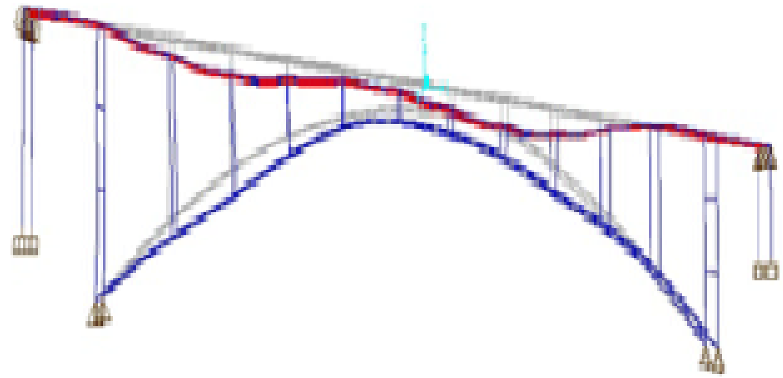

Fig. 6: Bridge deformation in mode no. 6 with frequency period 0, 482444 s-main mode-vertical vibration

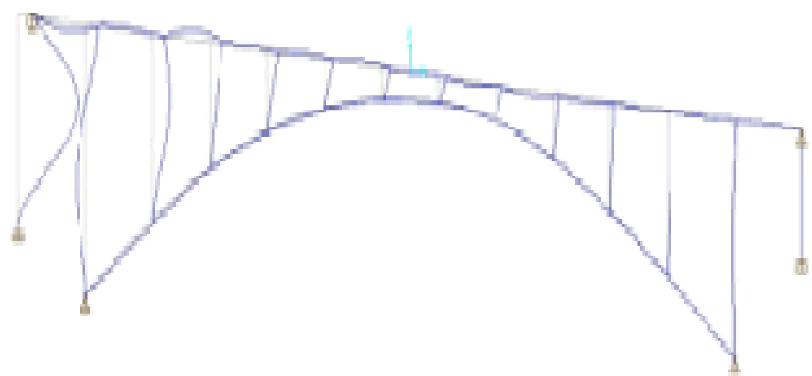

Fig. 7: Bridge deformation in mode no. 29 with frequency period 0, 198806 s-main mode-longitude vibration

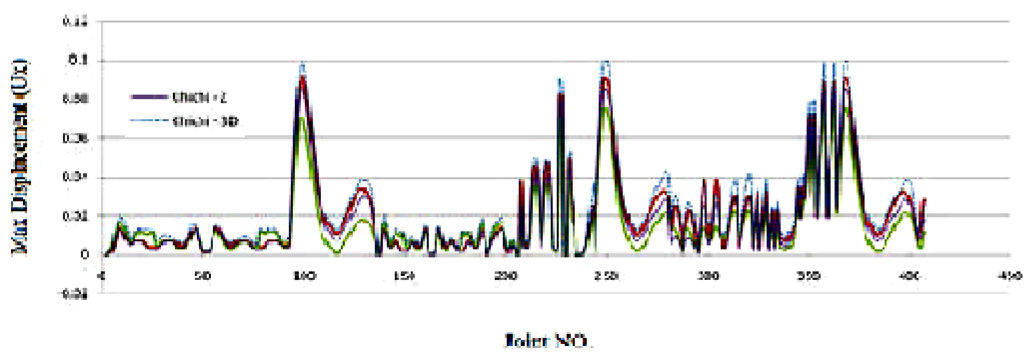

Fig. 8: Comparison of maximum displacement in the longitude direction in analyses

Time history analysis: For time history analysis of acceleration records of earthquakes of Tabas, Northridge, Chi Chi has been used in three directions. First, one component analysis and then, three-component analysis have been conducted.

RESULTS AND DISCUSSION

Comparison of maximum displacement in the longitude, traverse and vertical directions in one-component and three-component analyses: Comparison of maximum absolute displacement of the joints in longitude direction in one-component and three-component analyses is shown in Fig. 8. Also comparison of maximum absolute displacement of the joints in traverse direction in one-component and three-component analyses is shown in Fig. 9. In addition, Comparison of maximum displacement of the joints in vertical direction is shown in Fig. 10.

Clearly, maximum displacement in longitude direction under the horizontal component of acceleration record is higher than other components. Moreover, the results of

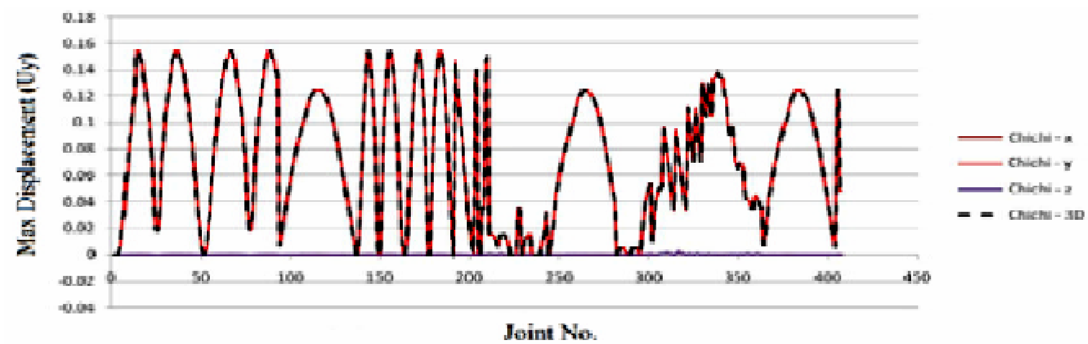

Fig. 9: Comparison of maximum displacement in the traverse direction in analyses

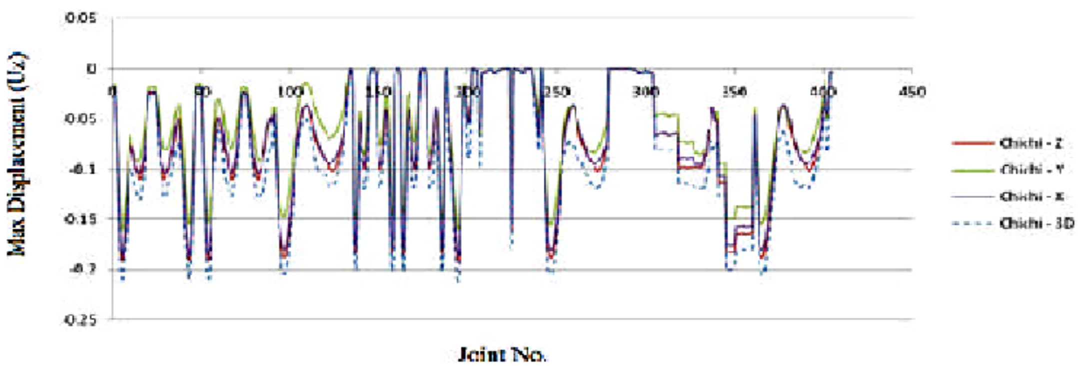

Fig. 10: Comparison of maximum displacement in the vertical direction

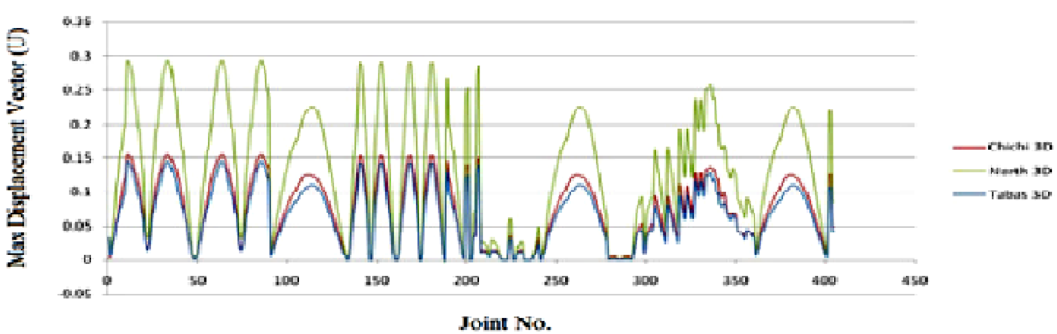

Fig. 11: Comparison of maximum displacement in three earthquakes

one-component analysis in longitude direction overlap with the results of the three-component analysis of the acceleration record with a satisfying precision. Based on the above diagram, in order to obtain the maximum traverse displacement, one-component analysis in traverse direction of the acceleration record can be used. In addition, it is clear than vertical and longitude components of the acceleration record cause trivial traverse displacement in the bridge.

Results of one component analysis in traverse direction overlap with the results of the three-component analysis of the acceleration record with a satisfying precision. Maximum displacement in vertical direction in one-component analyses occurs in an analysis under the vertical component of the acceleration record. Likewise, traverse component of the earthquake causes the minimum vertical displacement. Obtained results of the three-component analysis are 5-6% higher than the maximum values in one vertical one-component analysis of acceleration record.

Comparison of maximum displacement vector in three earthquakes: As shown in Fig. 11, maximum obtained values in three-component analysis of the Northridge

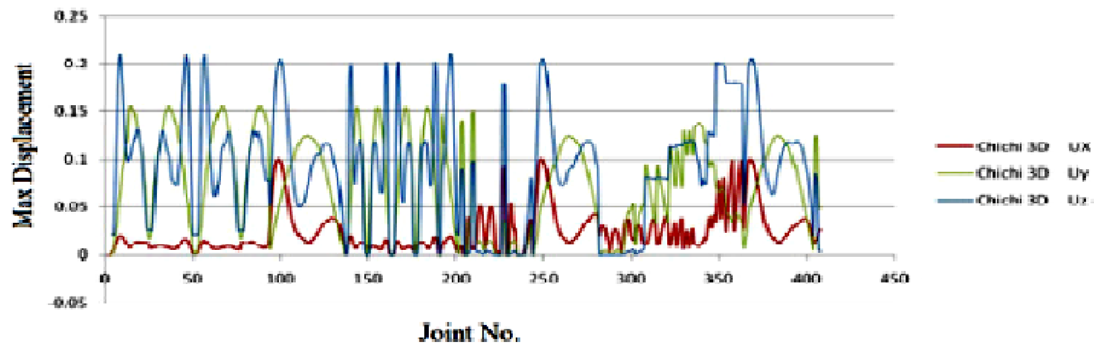

Fig. 12: Comparison of maximum displacement in three directions

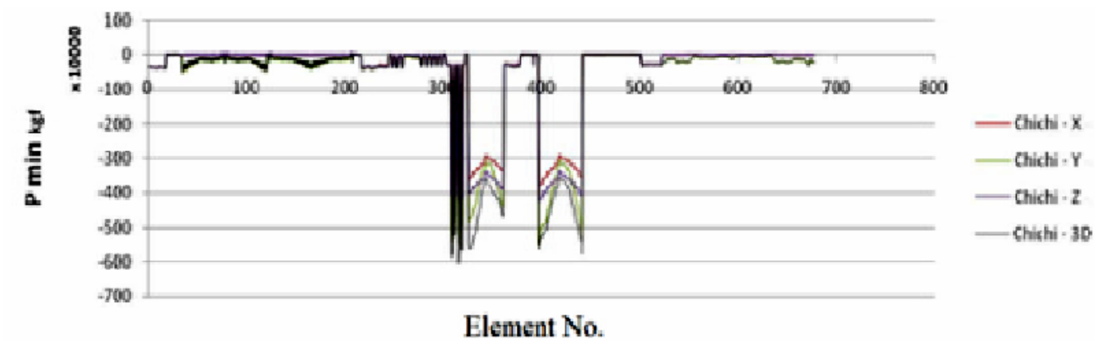

Fig. 13: Comparison of maximum axial pressure force (Pmin) in one-component and three-component analyses

earthquake are two-fold higher than the obtained maximum displacement values from two earthquakes of Tabas and Chi Chi. Also, the vibration behavior of the bridge is identical in these three earthquakes.

Comparison of maximum values of displacement in three directions with three-component analysis As shown in Fig. 12, maximum displacement in three-component earthquake of Chi Chi occurs in vertical direction and then in traverse direction.

Comparison of maximum axial force in one-component and three-component analyses: Maximum axial force in one-component analyses has occurred under the traverse component of Chi Chi earthquake (Fig. 13). Furthermore, obtained responses from the traverse analysis shows the trivial difference (<2%) with one-component analysis (traverse component of the acceleration record).

Comparison of maximum axial force in three-component analyses: As shown in Fig. 14, Maximum axial pressure forces have occurred in Northridge, Tabas and Chi Chi in the elements, respectively.

Comparison of the values of the support reaction: At the beginning of the analysis, resultant traverse force of the support is zero. This value changes with beginning the analyses. Maximum value of this force has occurred in Northridge earthquake. This shows that the value of traverse component of Northridge earthquake is higher than other earthquakes. Moreover, it is clear that longitude component and vertical component have the trivial effects on causing the traverse force (Fig. 15.). At the beginning of the analysis, resultant vertical force of the support is equal to the sum of the gravity loads (weight of the structure as well as sum of the live and dead loads). This value changes with beginning the analyses. Maximum value of this force has occurred in Tabas earthquake. Moreover, it is clear that longitude component and traverse component have the substantial effects on causing the vertical force (Fig. 16 and 17).

Values of vertical force on the support induced by the above-mentioned earthquakes compared to traverse force and longitude force is 3 and 6 fold, respectively.

Clearly, maximum vertical force in the support is higher than other forces but the amplitude of the changes

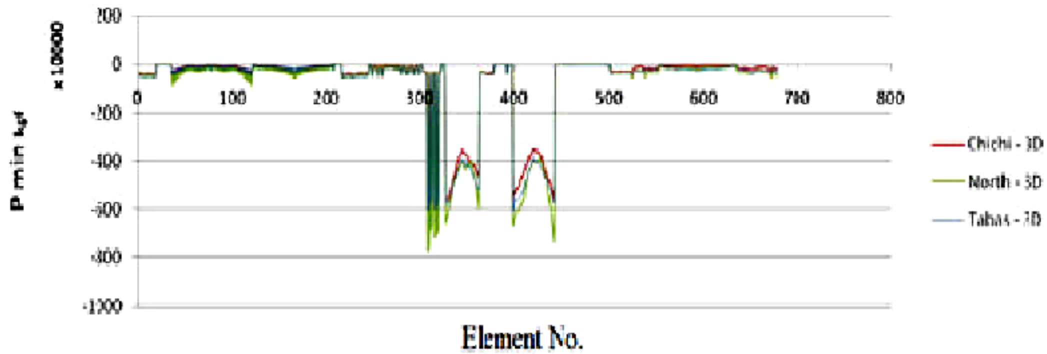

Fig. 14: Comparison of maximum axial pressure force (Pmin) in three-component analyses

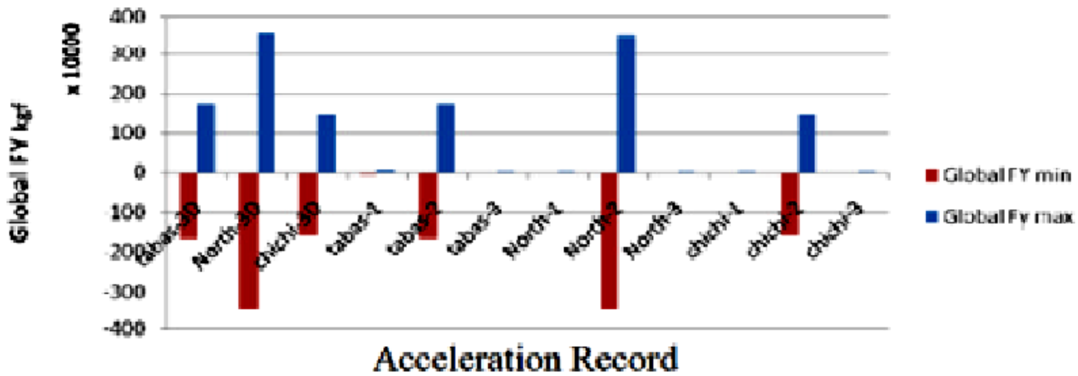

Fig. 15: Comparison of the values of the support traverse reaction

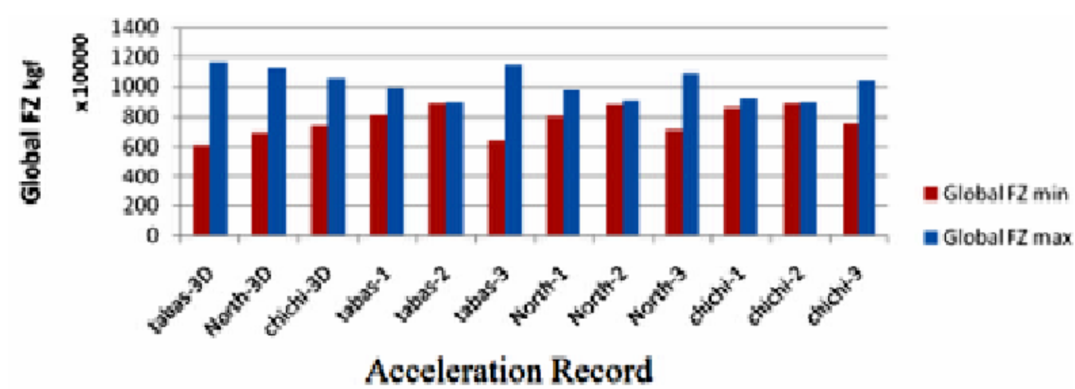

Fig. 16: Comparison of the values of the support vertical reaction

shows that the effect of traverse component in causing the force in the support is higher than other components.

Results of static analysis of the extended live and dead loads: Maximum displacement in the main arch near the support is 0.15 m and maximum axial force occurs in main arch near the support.

Results of time history analysis: Generally, longitude component of the acceleration record causes the highest longitude displacement, traverse component of the acceleration record causes the highest traverse displacement and the obtained results of their one-and three-component analyses are similar. Three-component analysis causes the highest vertical displacement.

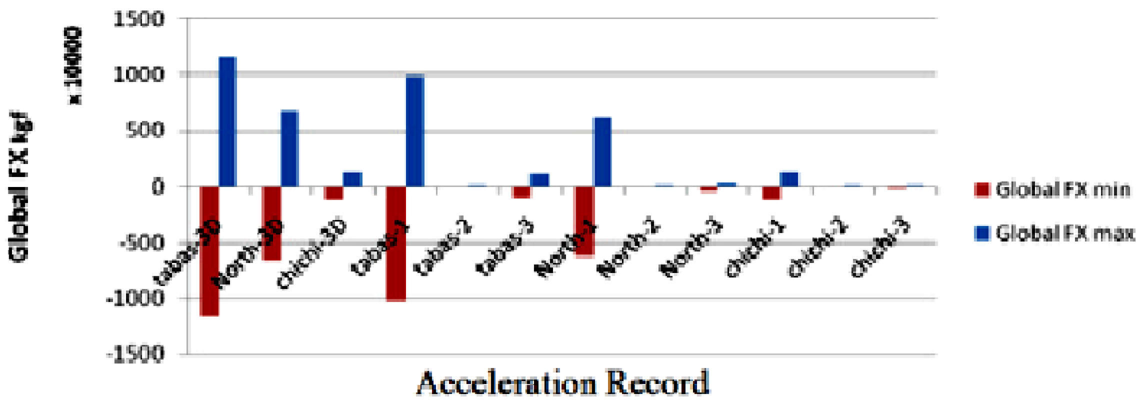

Fig. 17: Comparison of the values of the support longitude reaction

CONCLUSION

Under the effect of vertical component of the earthquake, the values of the maximum displacement can increase up 7%. Moreover, values of the axial force of the three-component analysis are the highest. These values differ from the values obtained from the one component vertical analysis.

REFERENCES

Kawashima, K. and A. Mizoguti, 2000. Seismic response of a reinforced concrete arch bridge. Proceedings of the 12th World Conference on Earthquake Engineering, January 30-February 4, 2000, Auckland, Nueva Zelanda.

Kuranishi, S. and A. Nakajima, 1986. Strength characteristics of steel arch bridges subjected to longitudinal acceleration. JSCE Structural Eng. Earthquake Eng., 3: 287-295.

Okumura, T., Y. Goto and K. Ozawa, 2000. Ultimate in-plane behavior of upper-deck type steel arch bridges under seismic loads. J. Struct. Eng., 46: 1333-1342.

Sakakibara, Y., K. Kawashima and G. Shoji, 1998. Analytical evaluation of an upper-deck type two-hinge steel arch bridge. J. Struct. Eng., 44: 761-767.

Torkamani, M.A.M., 2002. Dynamic behavior of steel deck tension-tied arch bridges to seismic excitation. Ournal of Bridge Engineering (ASCE), Auckland, New Zealand.

Yanagi, T., A. Nakajima and I. Saiki, 2003. Two-dimensional elasto-plastic behavior of deck type steel arch bridge and its modeling. J. Struct. Eng., 49: 543-552.